Available online at www.sciencedirect.com
SCIENCE DIRECT®
Journal of Sound and Vibration 276 (2004) 689–711
JOURNAL OF SOUND AND VIBRATION
www.elsevier.com/locate/jsvi

Damping of flexural vibration in the plane of lamination of elastic–viscoelastic sandwich beams

Samir A. Nayfeh*

Department of Mechanical Engineering, Massachusetts Institute of Technology, 77 Massachusetts Avenue, Cambridge, MA 02139, USA

Received 17 September 2002; accepted 5 August 2003

Abstract

Laminated beams with internal viscoelastic layers are known to exhibit potentially high damping of flexural vibration in the direction normal to the plane of lamination. In this paper, a model is developed for vibration parallel to the plane of lamination of a symmetric five-layer elastic–viscoelastic sandwich beam. The model is used to study the resonant frequencies and damping ratios of the lowest several modes of beams with various boundary conditions and inertia and stiffness properties as the shear stiffnesses of the viscoelastic layers are varied. Experimental results for free–free beams with contiguous and segmented constraining layers are in reasonable agreement with the predictions of the model.

Significant damping can be attained in the lowest several modes in the plane of lamination of a sandwich beam if the boundary conditions on the principal and constraining layers differ. For the particular example of a partially covered cantilever with a square box-beam cross-section, it is found that a constrained-layer damping treatment whose mass is approximately 15% of the mass of the cantilever can produce loss factors larger than 0.07 in the first mode of vibration in both the direction normal to and the direction parallel to lamination.

1. Introduction

It is well known that a sandwich beam consisting of alternating elastic and viscoelastic layers can be designed to exhibit large damping of flexural vibration in the direction normal to the plane of lamination (the xy plane in Fig. 1). The potential of this so-called constrained-layer damping was recognized more than 40 years ago by Plass [1] and Kerwin [2]. The theoretical foundation for much of the work that followed was laid by Ross et al. [3] who analyzed the vibration of a three-layer sandwich beam under sinusoidal deflections. Since then, various researchers have

*Tel.: +1-617-253-2407; fax: +1-617-253-7549.
E-mail address: nayfeh@mit.edu (S.A. Nayfeh).

0022-460X/$ - see front matter © 2003 Elsevier Ltd. All rights reserved.
doi:10.1016/j.jsv.2003.08.034

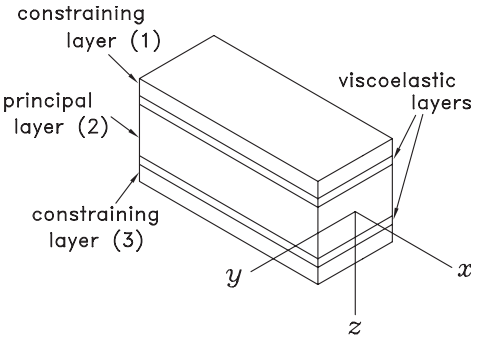

Fig. 1. Sketch of a five-layer symmetric sandwich beam.

extended the theory to include various boundary conditions [4–6], segmented and multiple constrained layers [7], and a host of other geometries as summarized in the review by Torvik [8].

The theory has also been extended to account for higher order effects such as rotary inertia and shear deformation (e.g., Refs. [9,10]). Other researchers have presented simplified analyses for design along with fabrication methods for internal shear dampers [11,12]. In recent years, a number of studies have focused on the construction of damped sandwich structures with anisotropic layers (e.g., Ref. [13]) or active layers (e.g., Ref. [14]). Sattinger [15] designed constrained-layer damping treatments for non-planar local and global vibration of structures made up of thin-walled circular tubes. Demoret [16] further optimized the shape of the constraining layers on circular tubes to damp torsional vibration.

In this paper, we develop a model for vibration of a symmetric five-layer elastic–viscoelastic beam in the plane of lamination (the xy plane in Fig. 1). A qualitative study of the nature of the vibration leads to a set of modelling assumptions that are employed to write a simple set of equations governing coupled vibration of the principal and constraining layers of the beam. For a beam with each layer simply supported, we write exact solutions and study the behavior of the beam as the shear stiffness of the viscoelastic layers is varied. Other boundary conditions are most readily studied using numerical solutions; we discretize the governing equations using the finite-element method and present results for beams with mixed boundary conditions and segmented constraining layers.

We show that significant damping can be obtained if the bending stiffness, inertia, and boundary conditions of the constraining layers differ from those of the principal layer of the beam. Experimental results are given for a few examples, and are in reasonable agreement with predictions based on the model. Finally, for the example of a partially covered cantilever box beam, we design a constrained-layer damping treatment to damp the first mode of vibration in both the direction normal to and the direction parallel to the plane of lamination. The numerical results indicate that it is practical in some cases to use a single set of constraining layers to damp non-planar flexural vibration.

2. Modelling

When a sandwich beam, such as the one shown in Fig. 1, vibrates in its plane of lamination, the elastic layers need not deflect together and significant strains can be induced in the viscoelastic

layers, resulting in potentially high damping. In this section, we develop a picture of the deformations and stresses that arise in such motion and obtain estimates of their relative magnitudes.

2.1. Lumped-parameter analogy

A lumped-parameter analogy for vibration in the plane of lamination of a sandwich beam such as that shown in Fig. 1 can be obtained by lumping the mass and stiffness of each layer as shown in Fig. 2.

The effective mass and flexural stiffness of the principal layer are lumped into m_2 and k_2. Likewise, we model the first constraining layer as an effective mass m_1 and flexural stiffness k_1 and the second as m_3 and k_3. Although the viscoelastic layers have negligible mass, they act as springs k_{12} and k_{23} that couple the elastic layers.

For a symmetric laminate such as that shown in Fig. 1, we have $k_1 = k_3$, $m_1 = m_3$, and $k_{12} = k_{23}$; and the mode shapes of the structure will be either symmetric or antisymmetric. If for the moment we consider k_{12} to be real, the mode shapes can be visualized as in Fig. 3.

The mode shape labelled (d) consists of antisymmetric motion of the constraining layers while the principal layer is still. In (c) the principal layer and constraining layers move in opposite phase. Now consider the case where the viscoelastic layers are reasonably stiff and moderately lossy (so that the mode shapes change little). Both modes (c) and (d) impart a great deal of strain energy into the viscoelastic layer and hence correspond to high-frequency, well-damped modes. The mode shape in (b), on the other hand, corresponds to a relatively low-frequency resonance with somewhat less damping. Here, the largest displacement belongs to the principal layer and hence we refer to such modes as "principal modes." It is our primary goal to develop an accurate model of these modes.

2.2. Coupling of bending and twist

In general the elastic layers that make up a beam like that shown in Fig. 1 do not bend together in the xy plane, and their relative motion produces a shearing stress in the viscoelastic layers. These shearing stresses act in such a way as to produce a twisting moment on the elastic layers, in effect coupling bending and twist of the composite beam. In the following, we estimate the angle

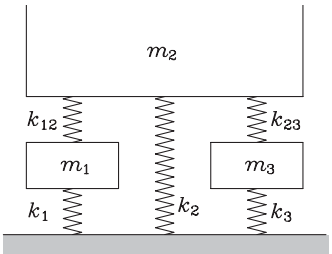

Fig. 2. Lumped-parameter model for vibration in the plane of lamination of a five-layer beam: The principal layer with effective mass m_2 is coupled via the viscoelastic layers with effective stiffnesses k_{12} and k_{23} to the constraining layers with effective masses m_1 and m_3.

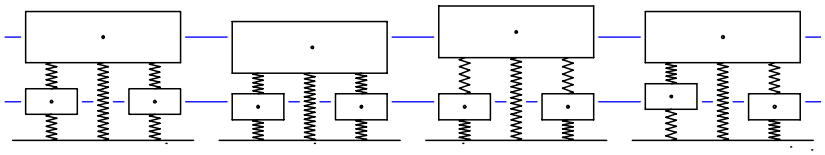

Fig. 3. Mode shapes from the lumped-parameter model of a symmetric five-layer laminate oscillating in its plane of lamination: (a) static configuration, (b) primary mode, (c) high-frequency symmetric mode, and (d) antisymmetric mode.

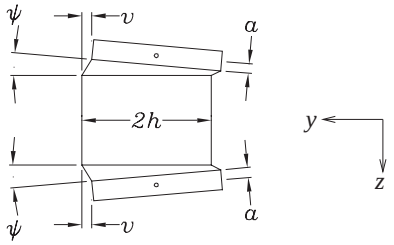

Fig. 4. Coupling of bending and twist in symmetric modes: A horizontal force applied at the centroid of a constraining layer results in the deflection v and rotation ψ relative to the principal layer.

of twist that results from displacement of one elastic layer relative to another and establish conditions under which the coupling between bending and twist can be ignored.

For symmetric modes, the principal layer will not twist at all, and we are concerned with rotation of the constraining layers relative to the principal layer. If we neglect the torsional stiffness of the constraining layers, we can treat the constraining layer as a rigid block on a compliant sheet as shown in Fig. 4. In response to a force applied at a distance a from the base of the viscoelastic material, we find that the displacement v scales with the rotation ψ according to

$$\frac{h\psi}{v} \sim \frac{3G(1-2\nu)(1+\nu)}{E(1-\nu)}\left(\frac{a}{h}\right), \tag{1}$$

where G, E, and ν are, respectively, the shear modulus, elongational modulus, and the Poisson ratio of the viscoelastic layer. In our problem, the distance a is the distance from the center of mass of the constraining layer to its base, and the quantity $h\psi$ is the magnitude of the vertical deflection at the edge of the constraining layer. Hence, as long as $a \ll h$, the deflection $h\psi$ due to twist is much smaller than the horizontal deflection v, and rotation of the constraining layer can be neglected. Even if this condition is not satisfied, we may still neglect rotation of the constraining layer if $\nu \approx \frac{1}{2}$, as is often the case for rubber-like viscoelastic materials.

2.3. Deformation in a viscoelastic layer

Assuming steady harmonic motion at an angular frequency $\bar{\omega}$, we let the transverse displacement in the y direction of the ith layer in Fig. 5 be $\mathrm{Re}(v_i(x)e^{j\bar{\omega}t})$, where j is the imaginary unit and $v_i(x)$ is a complex-valued function whose magnitude and phase correspond to the magnitude and phase of motion. For pure bending about the z-axis, if plane sections of the elastic

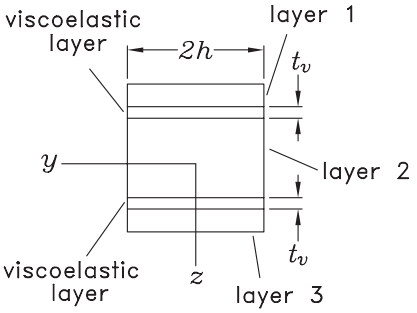

Fig. 5. Cross-sectional view of a sandwich beam showing the notation used in the analysis: the elastic layers are numbered sequentially from top to bottom, the width of the laminated section is $2h$, and each of the viscoelastic layers is of thickness t_v.

layers remain plane and normal to the neutral axis and the neutral axis does not extend, then the (harmonic) longitudinal deflection of a point in the elastic layer will be

$$u_i(x, y) = -y \frac{\partial v_i(x)}{\partial x}. \tag{2}$$

Then assuming that the shear strains do not vary through the thickness of a viscoelastic layer, they are given by

$$\gamma_{xy}(x, y) = 0, \tag{3}$$

$$\gamma_{xz}(x, y) = \frac{y}{t_v}\left[\frac{\partial v_i(x)}{\partial x} - \frac{\partial v_{i+1}(x)}{\partial x}\right], \tag{4}$$

$$\gamma_{yz}(x, y) = \frac{v_{i+1}(x) - v_i(x)}{t_v}. \tag{5}$$

We model the viscoelastic material as hysteretically damped without frequency dependence. This "ideal" hysteretic damping model is valid only for steady harmonic motion (e.g., Ref. [17]) and can be represented in the frequency domain by a complex stiffness. Hence, we introduce the complex shear modulus $G = G_v(1 + j\eta_v \operatorname{sgn} \bar{\omega})$ and the harmonically varying shear stresses in the viscoelastic layer are given by $\tau_{xz} = G\gamma_{xz}$ and $\tau_{yz} = G\gamma_{yz}$.

2.4. Summary of modelling assumptions

1. The principal and constraining layers are perfectly elastic, and the viscoelastic layers are frequency-independent hysteretic.
2. The principal and constraining layers obey the Euler–Bernoulli beam model; that is, rotary inertia as well as all components of shear deformation are neglected in the elastic layers.

3. The inertia of the viscoelastic layers is negligible. This is usually a safe assumption because the mass density of most damping materials is low in comparison with that of structural materials and most designs employ relatively thin viscoelastic layers.
4. The shear strain is constant through the thickness of a viscoelastic layer.
5. The normal stresses in the viscoelastic layers are negligible in comparison to the normal stresses in the principal and constraining layers. This assumption follows from the viscoelastic layers being subject to normal strains comparable to those in the elastic layers but having much lower elongational moduli.
6. The angle of twist is negligible in each layer of the composite beam.

2.5. Equations of motion

We now set forth equations of motion for a symmetric N-layer sandwich beam of width $2h$ and where all of the viscoelastic layers are of thickness t_v as shown in Fig. 5.

The ith elastic layer is characterized by flexural stiffness E_iI_i and mass per unit length ρ_iA_i. Denoting its harmonic deflection as $v_i(x)$, we obtain an equation of motion in the form

$$-\bar{\omega}^2\rho_iA_iv_i + E_iI_i\frac{\partial^4 v_i}{\partial x^4} + Q_i(x) - \frac{\partial R_i(x)}{\partial x} = 0, \tag{6}$$

where $Q_i(x)$ and $R_i(x)$ represent, respectively, the distributed force and moment exerted on the layer by adjoining viscoelastic layers. Integrating the shear-stress distribution given in Eqs. (3)–(5) over the width of the laminate, we obtain the net force per unit length,

$$Q_i(x) = -\frac{2Gh}{t_v}(v_i - v_{i+1}) - \frac{2Gh}{t_v}(v_i - v_{i-1}), \tag{7}$$

and bending moment per unit length,

$$R_i(x) = \frac{2Gh^3}{3t_v}\left(\frac{\partial v_i}{\partial x} - \frac{\partial v_{i+1}}{\partial x}\right) + \frac{2Gh^3}{3t_v}\left(\frac{\partial v_i}{\partial x} - \frac{\partial v_{i-1}}{\partial x}\right). \tag{8}$$

At the ends of each layer of the beam, we must specify four boundary conditions involving the displacement v_i, slope $\partial v_i/\partial x$, bending moment $E_iI_i\partial^2 v_i/\partial x^2$, and shear force

$$V_i = R_i - E_iI_i\frac{\partial^3 v_i}{\partial x^3}. \tag{9}$$

2.6. Dimensionless parameters

Designating the pth layer to be the principal layer, we define for the ith layer the mass and stiffness ratios

$$m_i = \frac{\rho_iA_i}{\rho_pA_p} \quad \text{and} \quad k_i = \frac{E_iI_i}{E_pI_p} \tag{10}$$

and rewrite Eqs. (6)–(8) in terms of dimensionless parameters as

$$-\omega^2 m_i v_i + k_i v_i^{\mathrm{iv}} = -g_v(2v_i - v_{i+1} - v_{i-1}) + g_m(2v_i'' - v_{i-1}'' - v_{i+1}''), \tag{11}$$

where the primes denote partial differentiation with respect to $\xi = x/L$ and L is the length of the beam. The dimensionless frequency ω is obtained by normalization of the frequency of motion $\bar{\omega}$ by a characteristic of the resonant frequencies of the principal layer in the absence of any other layers according to

$$\bar{\omega} = \frac{\omega}{L^2}\sqrt{\frac{E_p I_p}{\rho_p A_p}}. \tag{12}$$

The stiffness of the coupling among adjacent elastic layers is characterized by a displacement coupling parameter

$$g_v = \frac{2GhL^4}{t_v E_p I_p} \tag{13}$$

which is the dimensionless restoring force per unit length developed in a viscoelastic layer when the adjoining elastic layers undergo a unit relative deflection, and a rotation coupling parameter

$$g_m = \frac{2Gh^3L^2}{3t_v E_p I_p} = \frac{h^2}{3L^2}\, g_v \tag{14}$$

which is the dimensionless restoring moment per unit length developed in a viscoelastic layer when the adjoining elastic layers undergo a unit relative rotation.

3. Solution techniques

Our task now is to solve the eigenvalue problem posed by Eq. (11) along with appropriate boundary conditions. Exact analytical solutions are easily attained for only the simplest of boundary conditions, and we in general resort to either approximate analytical solutions or numerical methods.

3.1. Direct solution

The governing equations (11) constitute a set of constant-coefficient, linear, homogeneous equations of order $4N$, where N is the number of elastic layers. Therefore, unless an eigenvalue and eigenvector are repeated, the v_i will be of the form $A_i e^{\lambda x}$, where the A_i and λ are complex constants. If we substitute this form of solution into Eq. (11), we obtain the set of homogeneous algebraic equations

$$(g_v - \lambda^2 g_m)A_{i-1} + (k_i\lambda^4 - m_i\omega^2 + 2g_v - 2\lambda^2 g_m)A_i + (g_v - \lambda^2 g_m)A_{i+1} = 0 \tag{15}$$

which can be assembled into a matrix equation of the form

$$[D_1(\omega^2, \lambda)][A_i] = 0, \tag{16}$$

where the coefficient matrix $D_1(\omega^2, \lambda)$ yields a determinant of order $4N$ in the eigenvalue λ, so that for a given value of ω we can solve for the $4N$ values of λ that satisfy Eq. (11) and determine the eigenvectors A_i corresponding to each eigenvalue.

Denoting now the $4N$ eigenvalues and eigenvectors as λ_k and A_{ik} for $k = 1, 2, \ldots, 4N$, we can write the displacement $v_i(x)$ in the form

$$v_i(x) = \sum_{k=1}^{4N} V_k A_{ik} e^{\lambda_k x}, \tag{17}$$

where the V_k are complex constants. These displacements are required to satisfy $4N$ boundary conditions, which usually involve the $v_i(x)$ and their derivatives evaluated at the ends of the beam. If the boundary conditions are homogeneous, we can assemble them into the form

$$[D_2(\lambda_1, \lambda_2, \ldots, \lambda_{4N})][V_k] = 0, \tag{18}$$

where the dependence of D_2 on the λ_k is usually transcendental. Our task then is to find the value of ω and corresponding λ_k and A_{ik} for which the determinants of the matrices D_1 and D_2 are zero. Direct solution of such equations can be carried out with careful programming (e.g., Ref. [6]), but is especially difficult for many of the examples which we will consider in this paper because the eigenvalues coalesce for some parameter values.

3.2. Finite-element discretization

When developing approximate solutions to the eigenvalue problem posed by Eq. (11) with appropriate boundary conditions, we find it convenient to work from a variational formulation. Multiplying Eq. (11) by the virtual displacement $\bar{v}_i$, integrating over the length of the beam, and summing over i, we obtain

$$\sum_i \int_0^1 \bar{v}_i (k_i v_i^{\mathrm{iv}} - \omega^2 m_i v_i)\, \mathrm{d}\xi = \sum_i \int_0^1 \bar{v}_i [g_m(2v_i'' - v_{i+1}'' - v_{i-1}'') - g_v(2v_i - v_{i+1} - v_{i-1})]\, \mathrm{d}\xi. \tag{19}$$

For general boundary conditions, it is difficult to guess a set of global trial functions which give rapid convergence; we therefore discretize locally by the finite-element method. We treat the sandwich beam of Eqs. (19) as one element of a longer beam and approximate the deflection of the ith layer of this element as a cubic polynomial of the form

$$v_i(\xi) = \bar{v}_i(\xi) = \sum_{r=1}^{4} \phi_r(\xi) q_{ir}, \tag{20}$$

where q_{ir} is the rth element of the vector $q_i = [v_i(0), v_i'(0), v_i(1), v_i'(1)]^{\mathrm{T}}$ and the interpolation functions $\phi_r(\xi)$ are given by

$$\phi_1(\xi) = 1 - 3\xi^2 + 2\xi^3, \quad \phi_2(\xi) = \xi - 2\xi^2 + \xi^3, \tag{21, 22}$$

$$\phi_3(\xi) = 3\xi^2 - 2\xi^3, \quad \phi_4(\xi) = -\xi^2 + \xi^3. \tag{23, 24}$$

Substituting the expansion given by Eq. (20) into the variational Eq. (19), integrating by parts, and requiring that the resulting expression be stationary with respect to the q_{ns}, we obtain

the set of equations

$$-\omega^2 m_n \sum_{r=1}^{4} \langle \phi_r, \phi_s \rangle q_{nr} + k_n \sum_{r=1}^{4} \langle \phi_r'', \psi_s'' \rangle q_{nr}$$
$$= -\sum_{r=1}^{4} (g_v \langle \phi_r, \phi_s \rangle - g_m \langle \phi_r', \phi_s' \rangle)(2q_{nr} - q_{(n+1)r} - q_{(n-1)r}), \tag{25}$$

where $\langle f(\xi), g(\xi) \rangle = \int_0^1 f(\xi) g(\xi)\, d\xi$. This equation can be written in matrix form as

$$(K_n - \omega^2 M_n + 2G_v - 2G_m)q_n - (G_v - G_m)(q_{n+1} + q_{n-1}) = 0, \tag{26}$$

where the elements of the component matrices are defined as

$$(M_n)_{ij} = m_n \langle \phi_i, \phi_j \rangle, \quad (K_n)_{ij} = k_n \langle \phi_i'', \phi_j'' \rangle, \tag{27,28}$$

$$(G_v)_{ij} = g_v \langle \phi_i, \phi_j \rangle, \quad (G_m)_{ij} = g_m \langle \phi_i', \phi_j' \rangle. \tag{29,30}$$

The mass matrix M_n and stiffness matrix K_n are identical to the standard beam-element matrices found in many textbooks.

4. Examples

The boundary conditions imposed on motion in the plane of lamination of the sandwich beam can vary from layer to layer. Consider a simply supported beam to which are attached a pair of constrained-layer dampers. The ends of the constraining layers may be attached to the supports in the same manner as the principal layer, so that they too are simply supported in the plane of lamination. If instead the ends of the constraining layers are not attached to the supports at all, the boundary conditions imposed on the constraining layers are those of a free–free beam. We study these configurations and several others in the following examples.

4.1. Simple supports

In this section, we examine the dynamics of the sandwich beam for the particular case of a symmetric five-layer laminate where each of the principal and constraining layers is simply supported in the plane of lamination. Designating the second elastic layer to be the principal layer, we have $m_2 = k_2 = 1$. Because the laminate is symmetric, $m_1 = m_3 = m$ and $k_1 = k_3 = k$. For these boundary conditions, we can obtain exact solutions in the form

$$v_i(x) = a_{ir} \sin r\pi\xi. \tag{31}$$

Substitution of this expression into Eq. (11) for $i = 1, 2, 3$ yields

$$-\omega_r^2 m a_{1r} + k(r\pi)^4 a_{1r} = -\Gamma(a_{1r} - a_{2r}), \tag{32}$$

$$-\omega_r^2 a_{2r} + (r\pi)^4 a_{2r} = -\Gamma(2a_{2r} - a_{1r} - a_{3r}), \tag{33}$$

$$-\omega_r^2 m a_{3r} + k(r\pi)^4 a_{3r} = -\Gamma(a_{3r} - a_{2r}), \tag{34}$$

where

$$\Gamma = g_v + g_m(r\pi)^2. \tag{35}$$

Thus, corresponding to the rth mode of a decoupled simply supported beam, we have three modes of the composite beam, for which each layer deflects in the shape of the rth mode of a simply supported uniform beam.

Hence, for a given value of r, the motion of a composite beam on simple supports can be modelled using the lumped parameter model shown in Fig. 2. In Eqs. (32)–(34), the effective stiffness of the viscoelastic layers is measured by the parameter Γ, which we see from Eq. (35) is made up of a combination of the displacement-coupling parameter g_v and the slope-coupling parameter g_m. Recalling from Eq. (14) that $g_m = g_v(h^2/3L^2)$, we see that g_m can often be neglected for low values of r.

The eigenvalue problem given by Eqs. (32)–(34) is symmetric and hence admits two types of solution: antisymmetric modes with $a_{1r} = -a_{3r}$ and $a_{2r} = 0$ that satisfy

$$\omega_r^2 = \frac{\Gamma + k(r\pi)^4}{m} \tag{36}$$

and symmetric modes with $a_{1r} = a_{3r}$ that satisfy

$$m\omega_r^4 - [\Gamma(1+2m) + (r\pi)^4(k+m)]\omega_r^2 + [\Gamma(r\pi)^4(1+2k) + k(r\pi)^8] = 0 \tag{37}$$

and

$$[\Gamma + k(r\pi)^4 - m\omega_r^2]a_{1r} = \Gamma a_{3r}. \tag{38}$$

Modelling the behavior of the viscoelastic material as frequency-independent hysteretic, we set its complex shear modulus to $G = G_v(1 + \mathrm{j}\eta_v)$, where η_v is the loss factor of the viscoelastic material. Since Γ is proportional to G, we can write

$$\Gamma = \Gamma_r(1 + \mathrm{j}\eta_v). \tag{39}$$

For non-zero η_v, the resonant frequencies ω_r are complex valued, and the loss factor η of the composite beam is given by the ratio of the imaginary and real parts of the square of ω_r:

$$\eta = \frac{\mathrm{Im}(\omega_r^2)}{\mathrm{Re}(\omega_r^2)}. \tag{40}$$

In the following, we will discuss the effects of varying Γ_r and k for composite beams with lossy viscoelastic ($\eta_v = 1$) and constraining layers each with one-tenth the mass of the principal layer ($m = 0.1$).

For the case where $k/m = 1$ (where the natural frequencies of the decoupled principal and constraining layers are equal), the resonant frequencies are

$$\omega_r^2 = \left\{(r\pi)^4, (r\pi)^4 + \frac{\Gamma}{m}, (r\pi)^4 + \frac{\Gamma}{m}(1+2m)\right\} \tag{41}$$

from which we see that the first resonant frequency of the composite beam is equal to that of the individual layers and has $\eta = 0$. The principal mode in this case involves synchronous motion of the elastic layers of the beam. The two higher resonances are well damped for large η_v and Γ.

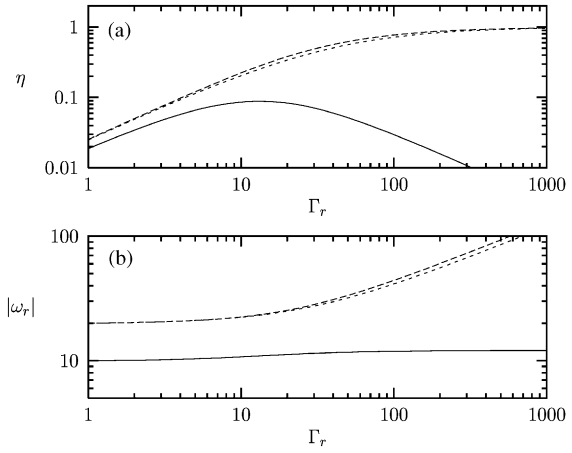

Fig. 6. Resonant frequencies (b) and composite loss factors (a) for $k/m = 4$ as a function of the real part of Γ for vibration in the plane of lamination of a five-layer symmetric laminate for $r = 1$, $\eta_v = 1.0$, and $m = 0.1$: principal mode (solid line), higher symmetric mode (short dashes), and asymmetric mode (long dashes). All layers of the beam are simply supported.

Next, we consider the case where $k/m > 1$ so that the natural frequencies of the decoupled constraining layers are higher than those of the principal layer. The resonant frequencies and loss factors are plotted as a function of Γ_r in Fig. 6. The two higher resonances are well damped for all but very low values of Γ_r. One of these resonances involves antisymmetric motion of the constraining layers and no motion of the principal layer, while the other involves symmetric motion of the constraining layers and relatively little motion of the principal layer.

Of greater practical interest is the first resonance, which involves large motion of the principal layer. The damping follows a trend similar to that observed for the planar shear damping mechanism: For small Γ_r, the principal and constraining layers are weakly coupled and large shear strains but little strain energy is imparted to the viscoelastic layers. For large Γ_r, the constraining layers are entrained to the principal layer and little shear strain occurs in the viscoelastic layers. Between these extremes, there exists a range of Γ_r over which significant damping (η as high as 0.09) can be obtained.

When $k/m < 1$, the natural frequencies of the decoupled constraining layers are lower than those of the principal layer. Consequently, as Γ_r is increased from a very low value (assuming $m < 0.5$), the two resonances given by Eq. (37) cross over as shown in Fig. 7. Near this crossover region, the behavior resembles that of a tuned-mass damper and loss factors greater than 0.2 can be obtained for all three resonances.

4.2. Pinned and free ends

Now consider vibration in the plane of lamination of a five-layer symmetric sandwich beam whose principal layer is simply supported but whose constraining layers are free. As in Section 4.1, we consider a beam whose two constraining layers are each one-tenth the mass of the principal layer and whose viscoelastic layers have a loss factor $\eta_v = 1$. We are concerned with only the

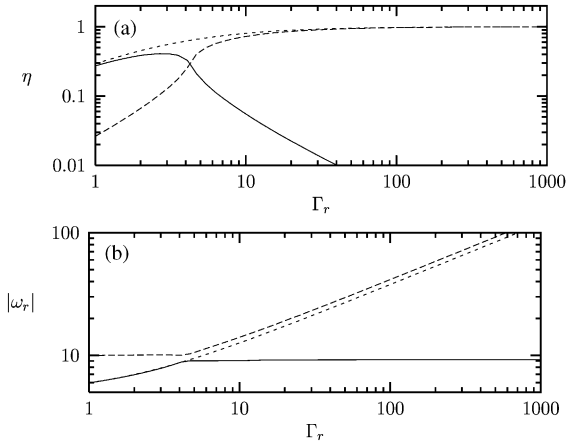

Fig. 7. Resonant frequencies (b) and composite loss factors (a) for $k/m = 0.25$ as a function of the real part of Γ for vibration in the plane of lamination of a five-layer symmetric laminate for $r = 1$, $\eta_v = 1.0$, and $m = 0.1$: principal mode (solid line), higher symmetric mode (short dashes), and asymmetric mode (long dashes). All layers of the beam are simply supported.

lowest few modes of the beam and hence we neglect the slope coupling g_m and plot the resonant frequencies and loss factors as functions of the real part of the displacement coupling parameter g_v. Moreover, because the antisymmetric modes of the laminate involve no motion of the principal layer, we solve for only its symmetric modes.

Let us first consider the case where the constraining layers have a higher stiffness per unit mass than the principal layer. The resonant frequencies and loss factors of the first six symmetric modes of the laminate vary with $\mathrm{Re}(g_v)$ as shown in Fig. 8. The behavior of the solutions on these plots is not simple, especially where two or more branches come together. Hence we do not connect them by lines, but rather plot each solution individually and label the various branches of the solutions so that the correspondence between the resonant frequencies and loss factors can be seen.

For very small g_v the principal and constraining layers of the beam behave as if they are decoupled: the resonant frequencies correspond to those of the individual layers, and the loss factors approach zero. The solutions along the branches labelled a and b in Fig. 8 correspond, respectively, to rigid-body translation and rotation of the constraining layers. Branches c, d, and f correspond to the first three modes of the simply supported principal layer. Branch e represents the first flexural mode of the constraining layers.

For very large g_v, the principal and constraining layers behave as if they are rigidly coupled. The resonant frequencies are those of a simply supported beam with normalized flexural stiffness $1 + 2k$ and mass per unit length $1 + 2m$. Thus, branches g through l correspond to the first six flexural modes of a simply supported beam.

Consider the principal mode, which at low g_v corresponds to branch c. As g_v is increased from roughly 1–7, the resonant frequency increases very slowly but the loss factor goes from less than 10^{-3} to greater than 0.3. At $g_v \approx 7$, this eigenvalue coalesces with that of the rigid-body mode of branch a and the branches g and m are born. On the plot of $\log|\omega|$ versus $\log g_v$, the branch m lies approximately on a straight line along which the frequency increases rapidly with g_v and the loss factor approaches unity. At $g_v \approx 700$ branch m ends and gives rise to branch i.

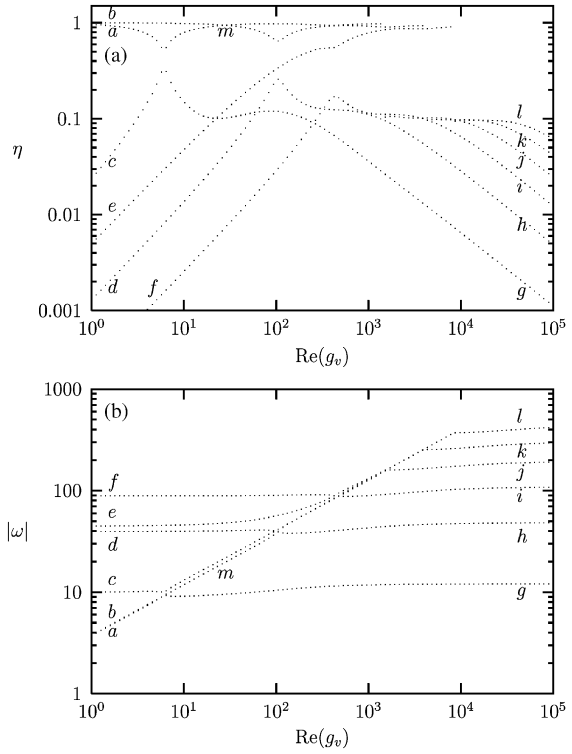

Fig. 8. Resonant frequencies (b) and loss factors (a) of the first six symmetric modes of vibration in the plane of lamination of a symmetric five-layer laminate: The principal layer is simply supported and the constraining layers are free, $m = 0.1$, $k/m = 4$, $\eta_v = 1$, and $g_m = 0$.

The response to a low-frequency disturbance is determined primarily by the resonant frequency and loss factor along the branches c and g. The highest damping is obtained at their intersection (at $\mathrm{Re}(g_v) \approx 7$) where $\eta \approx 0.3$ and $|\omega| \approx 10$. However, the damping near this intersection is very sensitive to changes in g_v and the damping along branch d is very light. It may therefore be advantageous to choose designs with $\mathrm{Re}(g_v)$ between 50 and 200, where the loss factors along both branches g and d are both greater than 0.1.

Next, consider the case where the constraining layers have lower stiffness per unit mass than the principal layer. The resonant frequencies and loss factors obtained from the finite-element model for the case $k/m = 0.25$ are plotted in Fig. 9.

The maximum damping of the principal mode in this case is comparable to that shown in Fig. 8 for the case $k/m = 4$, but it is attainable over a very narrow range of g_v. Moreover, whereas for $k/m = 4$ loss factors greater than 0.1 can be obtained along the branch g for values of $\mathrm{Re}(g_v)$ between 7 and 200, the loss factor in this case falls to below 0.1 at $\mathrm{Re}(g_v) = 11$.

We have seen in Section 4.1 that, when each elastic layer of the beam is simply supported, significant damping of the principal modes can be obtained only if the principal and constraining layers are detuned. But if the boundary conditions differ, then the principal modes are well damped (for appropriately chosen g_v) even for perfectly tuned principal and constraining layers.

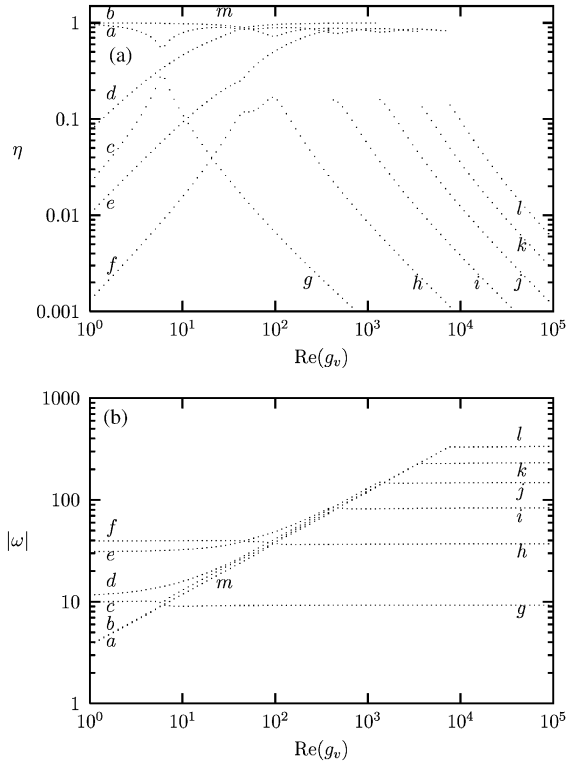

Fig. 9. Resonant frequencies (b) and loss factors (a) of the first six symmetric modes of vibration in the plane of lamination of a symmetric five-layer laminate: The principal layer is simply supported and the constraining layers are free, $m = 0.1$, $k/m = 0.25$, $\eta_v = 1$, and $g_m = 0$.

In Fig. 10, we plot the first six resonant frequencies and loss factors of a "perfectly tuned" ($k/m = 1$) laminate whose principal layer is simply supported but whose constraining layers are free. The damping behavior in this case is comparable to that found for the case $k/m = 0.25$.

4.3. Free ends

Let us now consider free–free vibration in the plane of lamination of the ceramic-viscoelastic beam with the cross-section shown in Fig. 11.

The principal layer is a box beam composed of 96% alumina ceramic with Young's modulus $E_1 = 311$ GPa and the constraining layers are 99.5% aluminum oxide with $E_2 = 372$ GPa. The viscoelastic layers are each 0.25 mm thick and composed of EAR-C1002 [18], which at 2000 Hz and room temperature has complex modulus $G_v = 13.9(1 + j0.95)$ MPa. The beam was suspended using light surgical tubing at points approximately one quarter of the beam length from each end. An impact hammer (PCB 086B03) provided an excitation close to the same end of the beam that an accelerometer (PCB 356B08) was mounted. Fifteen averages were collected using an HP365670A dynamic signal analyzer. The endpoint receptance measured in the y direction of the composite beam is plotted in Fig. 12.

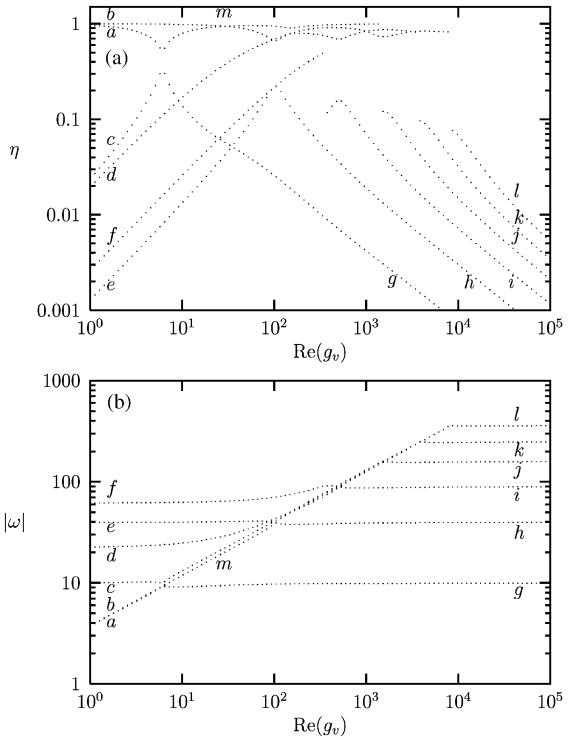

Fig. 10. Resonant frequencies (b) and loss factors (a) of the first six symmetric modes of vibration in the plane of lamination of a symmetric five-layer laminate: The principal layer is simply supported and the constraining layers are free, $m = 0.1$, $k/m = 1$, $\eta_v = 1$, and $g_m = 0$.

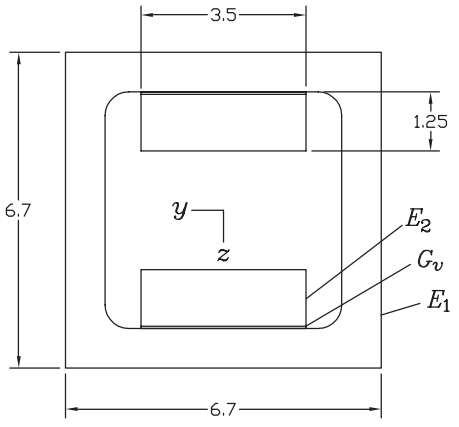

Fig. 11. Cross-section of a ceramic box beam with constrained viscoelastic layers: The beam is 0.914 m long and is composed of a principal layer with $E_1 = 311$ GPa, constraining layers with $E_2 = 372$ GPa, and viscoelastic layers with $G_v = 13.9(1 + j0.95)$ MPa and thickness 0.25 mm. Dimensions are in cm.

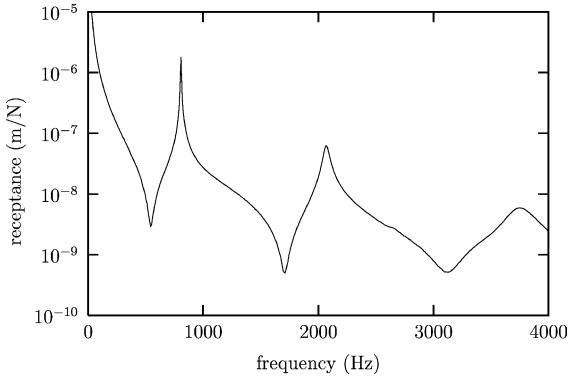

Fig. 12. Measured endpoint receptance in the plane of lamination of the ceramic beam of Fig. 11.

Table 1
Comparison of measured and predicted resonant frequencies and damping for the ceramic box beam of Fig. 11

Frequency (Hz)		Loss factor	
Measured	Predicted	Measured	Predicted
808	795	0.007	0.004
2065	2103	0.036	0.034
3730	3800	0.103	0.141

In terms of our non-dimensional parameters, the ceramic laminate has $m = 0.25$, $k = 0.055$, $\eta_v = 0.95$, and $g_v = 2160(1 + j0.95)$. The slope coupling g_m in this case is equal to $g_v/2000$ and can be safely ignored for the lowest several modes of the beam. The results of a finite-element calculation with these parameter values compare to the measured data as shown in Table 1.

The considerable error in the prediction of the loss factor of the first and third modes is probably due to the variation of the viscoelastic material properties with frequency. We use the material properties corresponding for 2000 Hz in our calculations although the shear modulus of the viscoelastic material (EAR C-1002) more than doubles as the frequency increases from 1000 to 3000 Hz. Moreover, according to Eq. (1), the displacement-normalized twist between elastic layers under symmetric motion scales with a/h, where a is half the thickness of the constraining layer and h is half its width. For the beam under consideration $a/h = 0.36$ so we cannot expect the model to predict the damping very accurately with such thick constraining layers.

It is perhaps interesting to see what damping (according to the model) would be achievable by adjusting g_v. In Fig. 13, we plot the resonant frequencies and loss factors of the beam as a function of the real part of g_v. From the plot, it is apparent that loss factors of better than 0.3 for any one mode could be achieved with proper selection of g_v, and that the current design with $g_v = 2160(1 + j0.95)$ is probably most effective for damping the third and fourth modes. A more compliant viscoelastic layer would yield better damping of the first two modes.

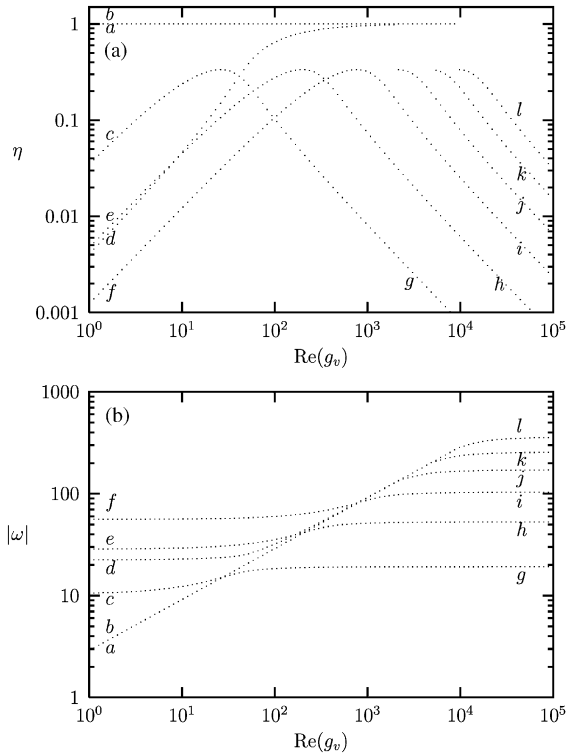

Fig. 13. Resonant frequencies (b) and loss factors (a) of the first six symmetric modes of vibration in the plane of lamination of the ceramic laminate of Fig. 11. The principal layer constraining layers have free ends, $m = 0.25$, $k/m = 0.22$, $\eta_v = 0.95$, and $g_m = 0$.

4.4. Free ends with segmented layers

Next, consider a free–free beam with the cross-section shown in Fig. 14, where the principal and constraining layers are solid aluminum bars. The stiffnesses per unit mass in the principal and constraining layers are equal so that $k/m = 1$ and we expect to obtain very little damping of the principal modes. The measured receptance (obtained using the same procedure as described in the previous section) is shown using a dotted line in Fig. 15; a least-squares curve fit to the resonant peaks indicates that η is less than 0.001 for the first two modes. Next, we segmented the constraining layers by making a transverse cut at the midpoint of the beam and repeated the measurement. The result is plotted with a solid line in Fig. 15, from which we see that segmentation of the constraining layers has caused a dramatic increase in the damping. In addition, we see that whereas the resonant frequency of the first mode has dropped, that of the second mode has increased.

Using a finite-element model with 10 elements, we obtain the plot of resonant frequency and loss factor as a function of g_{vr} shown in Fig. 16. The viscoelastic layer in the sample is composed of EAR-C3102 damping foam, which at room temperature and 500 Hz,

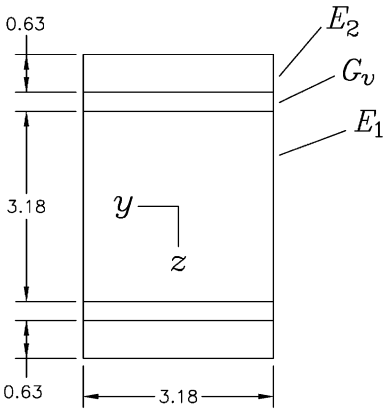

Fig. 14. Cross-section of an aluminum sandwich beam: The beam is 0.914 m long, and made up of solid aluminum bars bonded with a thin layer of epoxy to the intervening layers of EAR C-3102 damping foam. Dimensions are in cm.

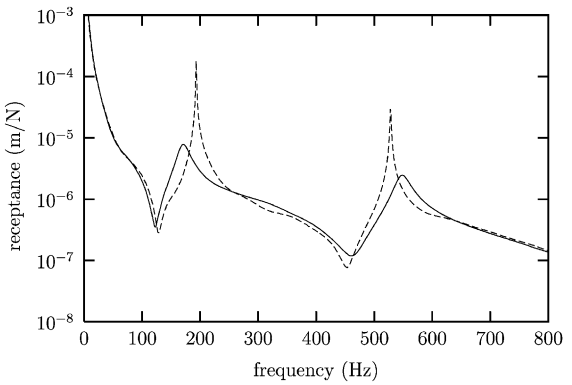

Fig. 15. Comparison of measured receptances for the sandwich beam of Fig. 14 with contiguous (dashed line) and segmented (solid line) constraining layers.

has $G_v = 0.1(1 + j1.0)$ MPa. Each viscoelastic layer is 0.25 inches thick; hence for our sample we have $g_v = 60(1 + j1.0)$. The results of the computation compare to curve-fitted experimental data as shown in Table 2. The agreement between the predicted and measured values is about as good as can be expected without taking into account the variation of the properties of the viscoelastic material with frequency.

4.5. Partially covered cantilever

We have seen that it is possible to obtain significant damping of low order modes of vibration in the plane of lamination of a sandwich beam. In this section, for the example of a cantilever box beam, we examine the possibility of designing a constrained-layer damping treatment to damp vibration in both the directions normal to and parallel to the plane of lamination.

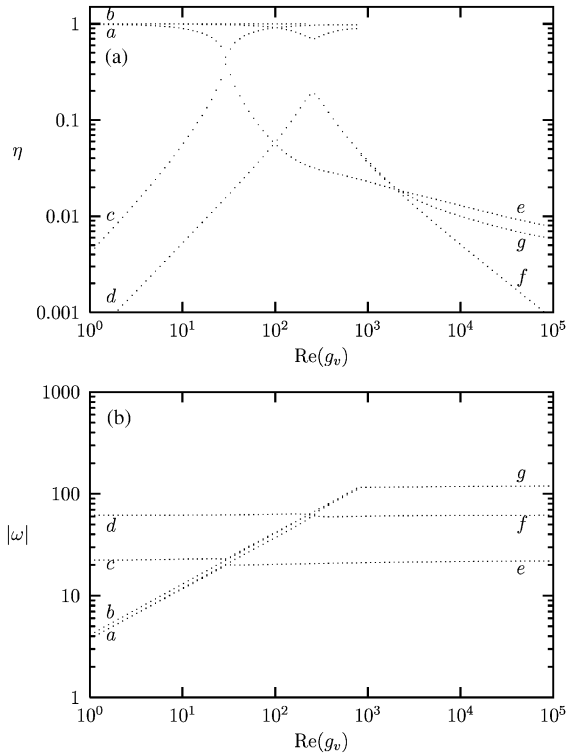

Fig. 16. Resonant frequency (b) and loss factor (a) for the first several symmetric modes of vibration in the plane of lamination of a symmetric five-layer laminate: The constraining layers are segmented at the midpoint of the beam, all ends are free, $m = 0.1$, $k/m = 1$, $\eta_v = 1$, and $g_m = 0$.

Table 2
Comparison of measured and predicted results

Frequency (Hz)		Loss factor	
Measured	Predicted	Measured	Predicted
170	175	0.092	0.103
547	550	0.040	0.035

According to the basic model, damping of vibration in the plane normal to lamination is governed by two dimensionless parameters (e.g., Ref. [5]). The "geometric parameter" Y is defined as

$$Y = \frac{2c^2 E_{cl} A_{cl}}{E_p I_p + 2E_{cl} I_{cl}}, \tag{42}$$

where c is the distance from the neutral axis of the principal layer to the center of mass of the constraining layers, $E_{cl}A_{cl}$ is the longitudinal stiffness of the constraining layers, E_pI_p and $E_{cl}I_{cl}$ are the bending stiffnesses in the z direction of the principal and constraining layers, respectively.

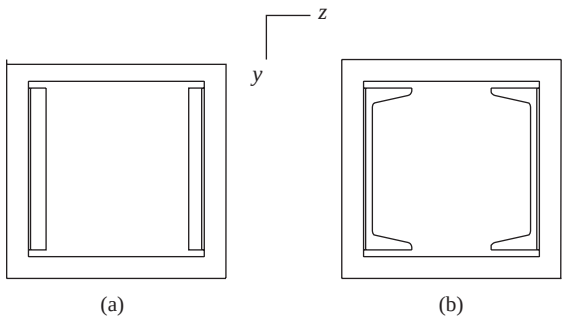

Fig. 17. Cross-section of a cantilever square box beam with internal constrained viscoelastic layers: the box has a length of 1.60 m, a width of 0.26 m, and a wall thickness of 12.5 mm. The constraining layers are (a) aluminum plates, and (b) steel channels.

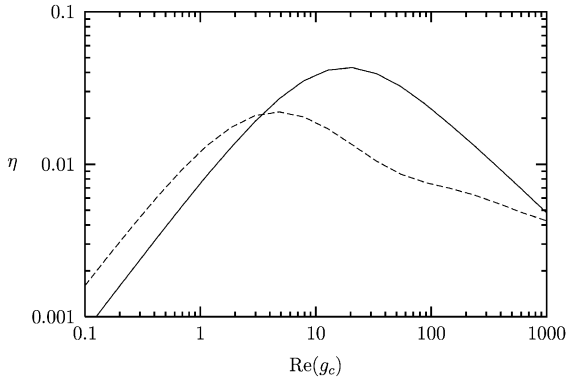

Fig. 18. Loss factor of the first mode in the x (solid line) and y (dashed line) directions of the partially covered cantilever with cross-section shown in Fig. 17(a) as a function of the real part of the coupling parameter g_c.

The "coupling parameter" g_c is a measure of the shear stiffness of the viscoelastic layers compared to the longitudinal stiffness $E_{cl}A_{cl}$ of the constraining layers. For a symmetric five-layer laminate, it is given by

$$g_c = \frac{GhL^2}{t_v E_{cl} A_{cl}}. \tag{43}$$

The governing equations are of sixth order, and are discretized using the finite-element method in a manner similar to that given in Section 3.2 (see Ref. [19]).

An aluminum cantilever beam with a square box-beam cross-section is shown in Fig. 17. We make use of constraining layers that extend over only the base quarter of the cantilever to damp the first mode of vibration in both the x and y directions. A first attempt at such a design is sketched in Fig. 17(a), where the constraining layers are made of aluminum plate with a thickness of 12.5 mm. In Fig. 18, the loss factor of the first mode in each of the x and y directions is plotted as a function of the real part of the shear parameter g_c associated with constrained layer damping of the column as defined in Eq. (43).

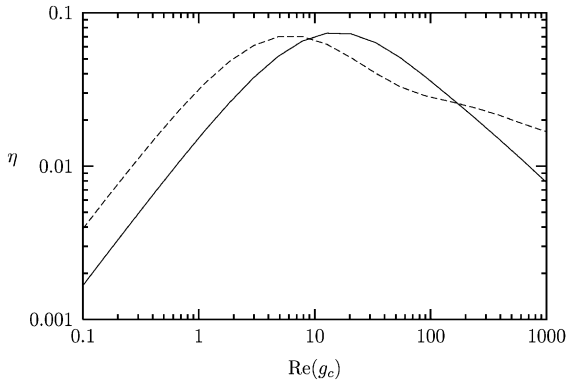

Fig. 19. Loss factor of the first mode in the x (solid line) and y (dashed line) directions of the partially covered cantilever with cross-section shown in Fig. 17(b) as a function of the real part of the coupling parameter g_c.

We see that while loss factors as high as 0.05 can be obtained in the x direction, the highest loss factor in the y direction is 0.02. Moreover, these maximum loss factors occur at different values of g_c, so we cannot simultaneously damp vibration in both directions. This damper performs so poorly because the constraining layers stiffen the beam only slightly in the y direction.

Let us consider as an alternative the use of steel channels (US standard C9 × 13.4) for the constraining layers as shown in Fig. 17(b). We obtain in this case the damping behavior shown in Fig. 19 with loss factors in both directions of about 0.07 for $\mathrm{Re}(g_c) = 10$. These constraining layers weigh approximately 25% more than those shown in Fig. 17(a) but yield three times greater damping in the plane of lamination.

5. Conclusions

In this paper, experimental evidence was presented that significant damping can be induced in low order modes of vibration in the plane of lamination of elastic–viscoelastic sandwich beams. A simple model for this vibration was developed, and its predictions are in reasonable agreement with the measurements. The model is based on the assumption that the angle of twist in each of the elastic layers is negligible, and hence is most accurate for beams with thin constraining layers mounted on opposing faces of a principal layer. According to the model, the damping in the composite beam depends on the ratio of the masses and stiffnesses of the constraining layers to the mass and stiffness of the principal layer, the coupling parameters g_v and g_m, and the boundary conditions on the various layers. For the lowest several modes of a slender beam, the slope coupling g_m can be neglected in comparison to g_v.

If the boundary conditions on the elastic layers are identical, the system behavior can be adequately modelled using a lumped parameter model such as shown in Fig. 2, and the behavior can be divided into three cases according to the tuning between the elastic layers: If the principal and constraining layers have the same stiffness per unit length, the principal mode is essentially undamped for any value of g_v. If the constraining layers have a higher stiffness to mass ratio than

the principal layer, their inertia plays only a small role in the dynamics, and the behavior as g_v is varied follows a trend like that of constrained-layer damping in the plane normal to the plane of lamination. On the other hand, if the constraining layers have a lower stiffness to mass ratio than the principal layer, the constraining layers can act as distributed tuned-mass dampers for some range of g_v.

If the boundary conditions on the principal and constraining layers differ, the variation of the resonant frequencies and damping ratios with changes in g_v are somewhat more complicated than can be captured with a lumped-parameter model. Because the mode shapes of the decoupled principal and constraining layers differ, the coupling forces are not distributed over the length of a layer in proportion to its decoupled mode shape, and the constraining layers can present to the principal layer a distributed impedance far higher than its lumped stiffness. Hence the potential exists for significantly higher damping than in beams where the boundary conditions on the principal and constraining layers are identical.

The behavior described in this paper is analogous to that attainable in the plane normal to lamination if transverse compression of the constrained layers plays an important role. The significance of transverse strains was first reported by Douglas and Yang [20] and later studied in more detail by Douglas [21], Miles and Reinhall [22], Sylwan [23], and Sisemore and Davernnes [24]. Because the viscoelastic materials incorporated in constrained-layer dampers are often nearly incompressible, relative motion parallel to the plane of lamination usually becomes important at lower frequencies than relative motion in the plane normal to lamination. Moreover, the bending stiffness of the constraining layers is often relatively large in the plane parallel to lamination, further enhancing the potential for damping of vibration in the plane of lamination.

For the particular example of a cantilever box beam, we have seen that a pair of constraining layers can produce high damping in both the directions normal to and parallel to the plane of lamination. This design requires significantly less mass than would be required if a pair of constraining layers is employed to damp vibration in each plane. Such configurations may also be useful when packaging constraints make it impossible to mount constraining layers on the surfaces normal to the plane of vibration.

References

[1] H. Plass, Damping vibrations in elastic rods and sandwich structures by incorporation of additional viscoelastic material, in: *Proceedings of the Third Midwestern Conference on Solid Mechanics*, 1957, pp. 48–71.

[2] E.M. Kerwin, Damping of flexural waves by a constrained viscoelastic layer, *Journal of the Acoustical Society of America* 31 (1959) 952–962.

[3] D. Ross, E. Ungar, E.M. Kerwin, Damping of plate flexural vibrations by means of viscoelastic laminae, in: J.E. Ruzicka (Ed.), *Structural Damping*, ASME, Atlantic City, NJ, 1959.

[4] R.A. DiTarantino, Theory of vibratory bending for elastic and viscoelastic layered finite-length beams, *Journal of Applied Mechanics* 87 (1965) 881–886.

[5] D.J. Mead, S. Markus, The forced vibration of a three-layer, damped sandwich beam with arbitrary boundary conditions, *Journal of Sound and Vibration* 10 (1969) 163–175.

[6] D.K. Rao, Frequency and loss factors of sandwich beams under various boundary conditions, *Journal of Mechanical Engineering Science* 20 (1978) 271–282.

[7] R. Plunkett, C.T. Lee, Length optimization for constrained viscoelastic layer damping, *Journal of the Acoustical Society of America* 48 (1970) 150–161.

[8] P.J. Torvik, The analysis and design of constrained layer damping treatments, in: P.J. Torvik (Ed.), *Damping Applications for Vibration Control*, AMD-Vol. 38, ASME, Chicago, IL, 1980.
[9] D.K. Rao, Vibration of short sandwich beams, *Journal of Sound and Vibration* 52 (1977) 253–263.
[10] Q. Chen, C. Levy, Vibration characteristics of partially covered double-sandwich beam, *American Institute of Aeronautics and Astronautics Journal* 34 (1996) 2622–2626.
[11] J.E. Ruzicka, Damping structural resonances using viscoelastic shear-damping mechanisms, *Journal of Engineering for Industry* 83 (1961) 414–424.
[12] E.R. Marsh, L.M. Hale, Damping of flexural waves with embedded viscoelastic materials, *Journal of Vibration and Acoustics* 120 (1998) 188–193.
[13] M.D. Rao, S. He, Dynamic analysis and design of laminated composite beams with multiple damping layers, *American Institute of Aeronautics and Astronautics Journal* 31 (1993) 736–745.
[14] A. Baz, J. Ro, Optimum design and control of active constrained layer damping, *Journal of Vibration and Acoustics* 117 (1995) 135–144.
[15] S.S. Sattinger, Constrained layer damping of global bending vibration modes of thin-walled beams, in: L. Rogers, J.C. Simonis (Eds.), *The Role of Damping in Vibration and Noise Control*, DE-Vol. 5, ASME, Boston, MA, 1987, pp. 33–40.
[16] K.J. Demoret, SPIE The barberpole: constrained-layer damping for bending and torsion, in: *Proceedings of Smart Structures and Materials 1995*: *Damping and Isolation*, Vol. 2445, San Diego, CA, 1995, pp. 350–361.
[17] S.H. Crandall, The hysteretic damping model in vibration theory, *Journal of Mechanical Engineering Science* 25 (1991) 23–28.
[18] E.A.R. Specialty Composites, Zionsville, Indiana, USA, Material Data Sheets.
[19] S.A. Nayfeh, Design and Application of Damped Machine Elements, Ph.D. Thesis, Massachusetts Institute of Technology, 1998.
[20] B.E. Douglas, J.C.S. Yang, Transverse compressional damping in the vibratory response of elastic–viscoelastic–elastic beams, *American Institute of Aeronautics and Astronautics Journal* 16 (1978) 925–930.
[21] B.E. Douglas, Compressional damping in three-layer beams incorporating nearly in-compressible viscoelastic cores, *Journal of Sound and Vibration* 104 (1986) 343–347.
[22] R.N. Miles, P.G. Reinhall, An analytical model for the vibration of laminated beams including the effects of both shear and thickness deformation in the adhesive layer, *Journal of Vibration, Acoustics, Stress, and Reliability in Design* 108 (1986) 56–64.
[23] O. Sylwan, Shear and compressional damping effects of constrained layered beams, *Journal of Sound and Vibration* 118 (1987) 33–45.
[24] C.L. Sisemore, C.M. Davernnes, Transverse vibration of elastic–viscoelastic–elastic sandwich beams: compression—experimental and analytical study, *Journal of Sound and Vibration* 252 (2002) 155–167, doi:10.1006/jsvi.2001.4038.